Published in : Thin-Walled Structures (2022), vol. 180, 109848
DOI: 10.1016/j.tws.2022.109848
Status : Postprint (Author's version)

CHARACTERIZATION OF UNSTIFFENED COLUMN WEBS IN TRANSVERSE COMPRESSION IN STEEL BEAM-TO-COLUMN JOINTS

Jean-Pierre Jaspart[1*], Adrien Corman[1], Jean-François Demonceau[1]

[1]*University of Liège, Belgium*

**University of Liège, Faculty of Civil Engineering, 9 Allée de la Découverte, B-4000 Liège, Belgium*

Abbreviations: CWC, Column web in compression

Keywords:

Steel joint, Component method, Column web in compression, Analytical model, Local buckling, Ductility

Abstract

The component method is widely used nowadays for the analytical prediction of the mechanical properties (rotational elastic stiffness, design resistance and ductility/deformation capacity) of steel and composite beam-to-column joints. The Part 1-8 of Eurocode 3 (EN 1993-1-8) provides expressions for the evaluation of the properties of many different joint components. However, a quick examination of EN 1993-1-8 highlights a glaring disproportion between the quantity of information related to rotational stiffness and plastic resistance, and that related to ductility and deformation capacity. For the latter, only few recommendations are provided, sometimes in line, and sometimes even not with the component approach itself. Present paper concerns one of these components, the ''column web in transverse compression'' (CWC), for which no information is basically available in terms of ductility. An original procedure for the prediction of the plastic deformation capacity is presented. It relies on a preliminary evaluation of the four main component properties : elastic stiffness, plastic resistance, post-plastic stiffness and ultimate resistance. Through this study, more accurate analytical formulae than those provided by EN 1993-1-8 for the evaluation of the plastic resistance are also suggested. All the developments are validated through extensive comparisons with already available experimental tests performed in various countries.

1. Introduction

Intensive research efforts have been devoted worldwide, during the last decades, to the study of the structural joints ; these ones have been progressively transferred into normative documents such as Eurocode 3 Part 1–8 (EN 1993-1-8) [1] in which calculation models are proposed for the evaluation of the mechanical properties of the joints (rotational stiffness, design resistance, ductility). However, a

Published in : Thin-Walled Structures (2022), vol. 180, 109848
DOI: 10.1016/j.tws.2022.109848
Status : Postprint (Author's version)

quick examination of EN 1993-1-8 highlights a glaring disproportion between the quantity of information related to rotational stiffness and plastic resistance, and that related to ductility and deformation capacity. For the latter, only few recommendations are provided, sometimes in line, and sometimes even not with the ''component approach'' [2] followed as general design philosophy in EN 1993-1-8. The same observation was made by other researchers [3]. This lack justified the launching of research projects at the University of Liège, which aim to develop analytical formulae for the evaluation of the deformation capacity of joint components so as to progressively fill the gap in knowledge and finally allow the designer to safely design structures and their joints at SLS and ULS, but also in case of exceptional events. These research projects are built upon the already existing scientific literature [4–6].

In this context, the present paper addresses the so-called ''column web in compression'' (CWC) component. This component is highlighted in **Fig. 1**(a) in the case of a typical single-sided beam-to-column joint with an extended endplate connection subjected to bending moment only. The typical response of the CWC component may be presented in the form of an $F - \Delta$ force–displacement curve (see **Fig. 1**(b)), where F and Δ designate the transversally acting compression force and the resultant shortening of the web, respectively. This latter is assumed to be measured in between the external face of the column flange and the column axis.

The shape of the $F - \Delta$ curve presented in **Fig. 1**(b) is globally bilinear and may be characterized by four key parameters: (i) an initial elastic stiffness K_{ini}, (ii) a ''plastic'' resistance F_{Rpl}, (iii) a strain-hardening (more generally post-plastic) stiffness K_{pp} and (iv) an ultimate resistance F_{Ru}. According to [2,7], the elastic resistance F_{Rel} may be simply estimated as 2/3 of F_{Rpl}.

In EN 1993-1-8, expressions are provided for the characterization of two out of the four key properties of the components, i.e. the initial stiffness K_{ini} and the ''plastic'' resistance F_{Rpl}. However, nothing is said in terms of strain-hardening (i.e. post-plastic) stiffness K_{pp} and ultimate resistance F_{Ru}; and, consequently, also in terms of ultimate deformation capacity Δ_u. On the basis of these two parameters ($^{K}_{ini}$ and $^{F}_{Rpl}$), a simplified bilinear $F - \Delta$ curve or a more complex trilinear $F - \Delta$ curve can be built, as shown in **Fig. 2**(a) and (b) respectively (see the solid blue curves). For these two curves, no limit is provided to the yield plateau. No further information on the actual ductility of the CWC component is added in Chapter 6.4 of EN 1993-1-8 dealing with joint rotation capacity.

In this paper, analytical procedures for the evaluation of the K_{pp} and F_{Ru} values on the basis of the component approach are proposed and validated against numerous experimental results. This will allow the designer to approximate the actual $F - \Delta$ curve, as shown in **Fig. 2**(a) and (b) (see the dashed red curves) and, in line with the objective of the present paper, to derive an estimation formula for the ultimate deformation capacity Δ_u. Subsequently, this one may be used to limit the length of the yield plateau in the EN 1993-1-8 approach.

Published in : Thin-Walled Structures (2022), vol. 180, 109848
DOI: 10.1016/j.tws.2022.109848
Status : Postprint (Author's version)

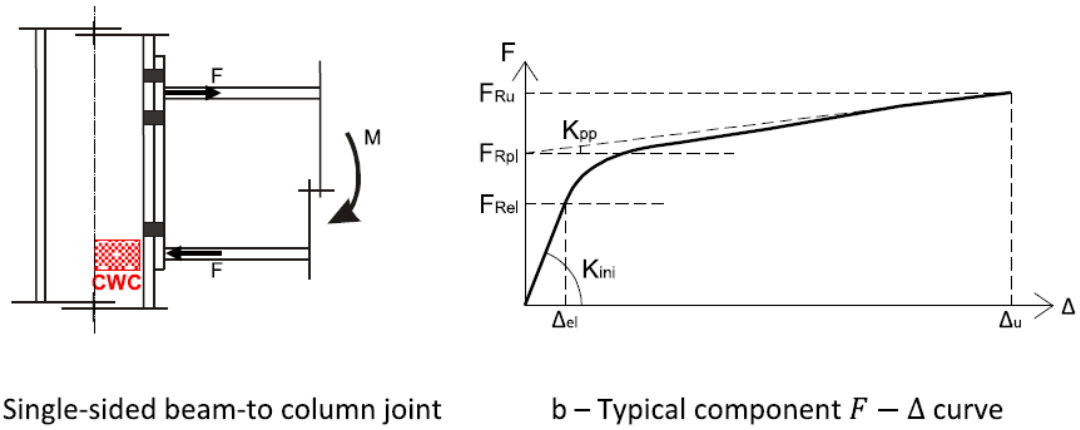

a - Single-sided beam-to column joint b – Typical component $F - \Delta$ curve

Fig. 1. CWC component.

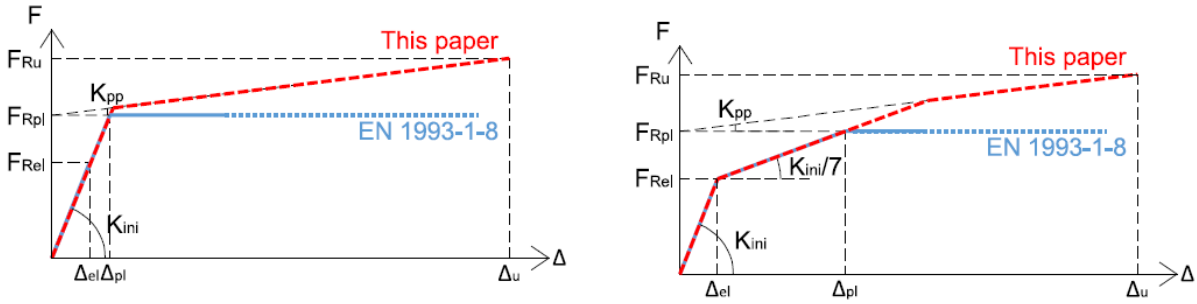

a – Bilinear approach b – Trilinear approach

Fig. 2. Simplified modelling of the CWC $F - \Delta$ curve.

2. Review of the EN 1993-1-8 model for the CWC component

2.1. ELASTIC STIFFNESS

The elastic initial stiffness K_{ini} of an unstiffened CWC component is obtained by multiplying the stiffness coefficient k_{ini} provided in EN 1993-1-8 by the Young's modulus of steel E, as expressed by **Eq. (1)**:

$$K_{ini} = ki_{ni}\ E \qquad (1)$$

where:

$$k_{ini} = \frac{0.7 \cdot \mathrm{b}_{eff,c,wc} \cdot \mathrm{t}_{wc}}{d_c} \qquad (2)$$

with:

- t_{wc} *:* the column web thickness;
- d_c : the clear depth of the column web;
- $b_{eff,c,wc}$ *:* the effective width of the column web in compression.

Published in : Thin-Walled Structures (2022), vol. 180, 109848
DOI: 10.1016/j.tws.2022.109848
Status : Postprint (Author's version)

The value of the clear depth d_c of the column may be computed through **Eq. (3)**, h_c being the column depth, t_{fc} the column flange thickness, r_c the root radius in hot-rolled column profiles and a_c the throat thickness of the welds connecting the flanges to the web in welded built-up column profiles:

$$d_c = \begin{cases} h_c - 2 \cdot (t_{fc} + r_c) & for\ a\ rolled\ I\ or\ H\ column\ profile \\ h_c - 2 \cdot (t_{fc} + \sqrt{2} \cdot a_c) & for\ a\ welded\ I\ or\ H\ column\ profile \end{cases} \quad (3)$$

The value of the effective width $b_{eff,c,wc}$ may be computed through **Eq. (4)** for either a welded or a bolted connection (see **Fig. 3**). This formula is a quite simplified version of a more complex one, initially presented in [7].

$$b_{eff,c,wc} = s + 5 \cdot (t_{fc} + r_c) \quad (4)$$

where s is defined by **Eq. (5)**, according to **Fig. 3**:

$$s = t_p + 2 \cdot t_e + 2\sqrt{2} \cdot a_p \quad (5)$$

2.2. PLASTIC RESISTANCE

According to EN 1993-1-8, the design plastic resistance of the CWC component may be expressed through **Eq. (6)**:

$$F_{c,wc,Rd} = \frac{\omega \cdot k_{wc} \cdot b_{eff,c,wc} \cdot t_{wc} \cdot f_{i,wc}}{\gamma_{M0}} \text{ but}$$

$$F_{c,wc,Rd} \leq \frac{\omega \cdot k_{wc} \cdot \rho \cdot b_{eff,c,wc} \cdot t_{wc} \cdot f_{y,wc}}{\gamma_{M1}} \quad (6)$$

In **Eq. (6)**:

- $f_{y,wc}$ is the material yield strength.
- ω is an interaction factor which differs from 1.0 when the column web is subjected, in addition to transverse compressive stresses σ_i, to significant shear stresses τ. This is the case for instance in the column web panel of a single-sided beam-to-column joint subjected to a bending moment or in the column web panel of a double-sided beam-to-column joint with unbalanced bending moments in the two connected beams.
- k_{wc} is a reduction factor covering the possible detrimental effect of the longitudinal compressive stresses σ_n coming from the axial force N_c and the bending moment M_c in the column. This effect has to be accounted for solely when the σ_n stresses exceed $0.7 \cdot f_{y,wc}$ in the column web (adjacent to the root radius for a rolled section or the toe of the weld for a welded section), as stated through **Eq. (7)**:

$$k_{wc} = \begin{cases} 1.0 & when\ \sigma_n \leq 0.7 \cdot f_{y,wc} \\ 1.7 - \frac{\sigma_n}{f_{y,wc}} & when\ \sigma_n > f_{y,wc} \end{cases} \quad (7)$$

Published in : Thin-Walled Structures (2022), vol. 180, 109848
DOI: 10.1016/j.tws.2022.109848
Status : Postprint (Author's version)

- ρ is a reduction factor accounting for the possible column web buckling and which may be defined through **Eq. (8)**, where $\bar{\lambda}_p$ is the reduced slenderness factor of the column web and may be defined through **Eq. (9)** as follows:

$$\rho = \begin{cases} 1.0 & if\ \bar{\lambda}_p \leq 0.67 \\ \frac{\bar{\lambda}_p - 0.22}{\bar{\lambda}_p^2} & if\ \bar{\lambda}_p \geq 0.67 \end{cases} \quad (8)$$

$$\bar{\lambda}_p = 0.932 \cdot \sqrt{\frac{\omega \cdot k_{wc} \cdot b_{eff,c,wc} \cdot d_c \cdot f_{y,wc}}{E \cdot t_{wc}^2}} \quad (9)$$

N.B.: for sake of accuracy, it was decided to consider, for **Eqs. (8)** and **(9)**, the new updated formulae which will be included in the forthcoming version of EN 1993-1-8. In **Eq. (8)**, the factor ''0.22'' replaced the incorrect original factor ''0.20'' (based on the well-known Winter formula) and so the limit slenderness factor has been adapted (i.e. ''0.67'' instead of ''0.72''). In addition, the k_{wc} and ω factors were introduced in **Eq. (9)**. These factors appeared in 1998 in a revised version of Eurocode 3 [8] and are based on research works achieved by Aribert et al. [9] and Jaspart [10], respectively.

- γ_{M0} and γ_{M1} are the so-called ''material'' safety factors, for resistance and instability respectively; their values are recommended in the National Application Document of the countries in which Eurocodes apply. In the present paper, these two coefficients will be systematically taken as equal to 1.0 as the aim is to compare new proposed formulae to experimental evidence (i.e. characteristic values of resistance $F_{c,wc,Rk}$ will be considered instead of design ones $F_{c,wc,Rd}$, see **Eq. (6)**).

For sake of convenience, in the following sections, the notation $F_{c,wc,Rk}$ will be used to refer to the formula of EN 1993-1-8 while a more simple F_{Rpl} one, will be used to refer to the new proposed formula (see Section 3).

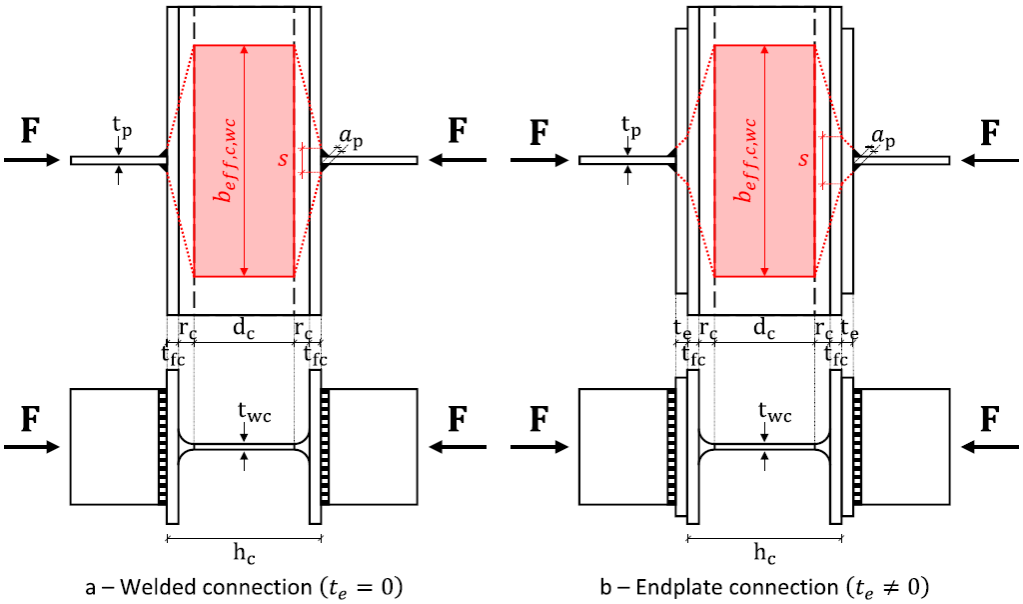

Fig. 3. Column web subjected to compression through transverse plates.

Published in : Thin-Walled Structures (2022), vol. 180, 109848
DOI: 10.1016/j.tws.2022.109848
Status : Postprint (Author's version)

2.3. COMPARISONS WITH EXPERIMENTAL DATA AND CONCLUSIONS

In order to highlight the capabilities of the EN 1993-1-8 model introduced in Section 2.2, a large database of 50 tests carried out in European [Rennes, Delft, Stuttgart and Liège] and American [Leigh and Waterloo] universities has been built [9,11,12], see **Table 1**. All the actual geometrical and mechanical properties of the specimens are reported in **Table 1**, when available (see the columns #2-#11 and the columns #12-#17, respectively). If not, the nominal properties are used.

Based on these values, it was possible to compute the EN 1993-1-8 behavioural properties of the CWC component for each individual test. This is done in **Table 2** (see the column #18 for K_{ini} and the column #24 for $F_{c,wc,Rk}$). This model has been graphically compared in **Fig. 4** to one of the tests presented in **Table 2** (i.e. the test *''CWC''* performed at the University of Liège). The tested specimen is presented in **Fig. 4**(a). It consists of a double-sided beam-to-column sub-assembly and it was designed and loaded in such a way that the CWC component is the only component activated. The experimental curve and the analytical prediction (following the bilinear approach depicted in **Fig. 2**(a)) are plotted in **Fig. 4**(b) in terms of $M - \phi$ curves (see the solid blue and black curves, respectively) since the CWC $F - \Delta$ curve was not made available in [12]. The following observations can be made from the comparison between the two:

- The initial stiffness is accurately captured by the analytical model;

- The plastic resistance is significantly underestimated by the analytical model. The experimental test is characterized by a column web buckling failure mode, which occurs in the elasto-plastic field, before strain-hardening develops. This is revealed by the absence of a clear bilinear response of the curve (such as the one presented in **Fig. 1**(b)), but also by the rather low decrease of the rotational stiffness under increasing bending moments. Therefore, the plastic resistance also corresponds to the ultimate resistance;

Based on these observations, it clearly appears that the EN 19931-8 formula for the evaluation of the plastic resistance of the CWC component (i.e. **Eq. (6)**) needs to be re-evaluated. This conclusion is confirmed by similar comparisons made with all the experimental tests reported in **Table 2**, which are characterized by a column web buckling failure mode occurring in the elasto-plastic range. These tests are highlighted in light blue in **Table 2**. For these tests, the ratio $F_{c,wc,Rk} / F_{Ru,exp}$ (see the column #25) is significantly lower than 1.0, with a mean value of 0.79 and a standard deviation of 0.07. This lack of accuracy will be addressed and improved in Section 3.1, this preliminary step being absolutely necessary for the subsequent characterization of the ultimate resistance (see Section 3.2) and of the deformation capacity (see Section 4) of this component.

Published in : Thin-Walled Structures (2022), vol. 180, 109848
DOI: 10.1016/j.tws.2022.109848
Status : Postprint (Author's version)

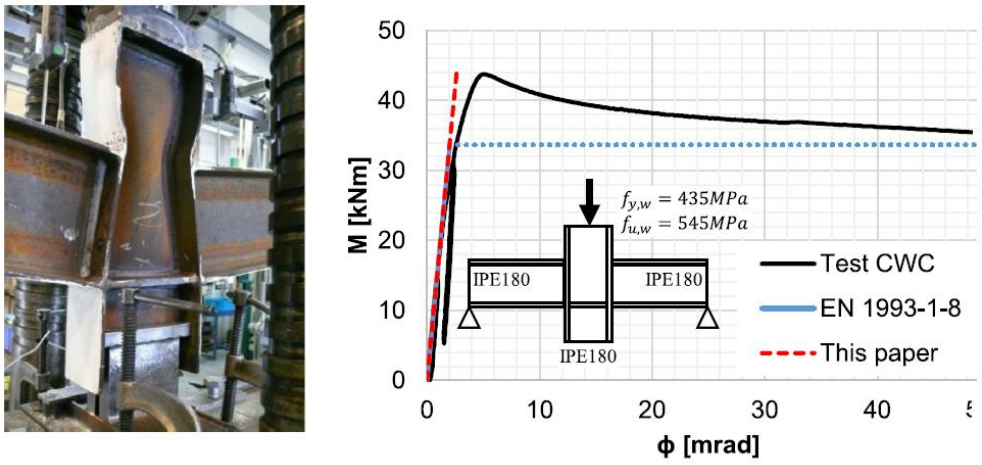

a – Tested specimen b - Experimental and analytical $M - \Phi$ curves

Fig. 4. Comparison between experimental and analytical results for the test *"CWC"*.

Table 1

Database of experimental tests – geometrical and mechanical properties.

EXPERIMENTAL DATA																	
Reference		Geometrical properties										Mechanical properties					
#0	#1	#2	#3	#4	#5	#6	#7	#8	#9	#10	#11	#12	#13	#14	#15	#16	#17
Author	Specimen	h_c (mm)	t_{wc} (mm)	t_{fc} (mm)	r_c (mm)	d_c (mm) *Eq. (3)*	t_p (mm)	t_e (mm)	a_p (mm)	s (mm) *Eq. (5)*	$b_{eff,c,wc}$ (mm) *Eq. (4)*	$f_{y,wc}$ (Mpa)	$f_{u,wc}$ (Mpa)	E (Mpa)	E_{pp} (Mpa)	$\sigma_n/f_{y,wc}$ (-)	$F_{Ru,exp}$ (kN)
Aribert et al. [6]	L1	140	7	12	12	92	10	0	5	24,1	144,1	320	–	210000	4200	0	365
	L2	200	9	15	18	134	10	0	5	24,1	189,1	320	–	210000	4200	0	770
	L3	260	10	17,5	24	177	10	0	5	24,1	231,6	320	–	210000	4200	0	870
	L4	140	7	12	12	92	20	0	10	48,3	168,3	320	–	210000	4200	0	375
	L5	200	9	15	18	134	15	0	8	37,6	202,6	320	–	210000	4200	0	780
	L6	200	9	15	18	134	20	0	10	48,3	213,3	320	–	210000	4200	0	825
	L7	260	10	17,5	24	177	20	0	10	48,3	255,8	320	–	210000	4200	0	880
Aribert,.., [6]	N1	160	8	13	15	104	15	0	8	37,6	177,6	275	397	210000	4200	0	550
Aribert et al. [6]	T1	200	9	15	18	134	15	10	8	57,6	222,6	265	411	210000	4200	0	760
	T2	200	9	15	18	134	15	15	8	67,6	232,6	265	411	210000	4200	0	800
	T3	200	9	15	18	134	15	20	8	77,6	242,6	265	411	210000	4200	0	840
	T4	200	9	15	18	134	15	30	8	97,6	262,6	265	411	210000	4200	0	940
Aribert et al. [6]	M1	141,9	5,1	6,4	7,8	113,5	10	0	5	24,1	95,1	303	416	210000	4200	0	175
	M2	255,3	7,8	11,8	23,8	184,1	15	0	8	37,6	215,6	335	459	210000	4200	0	608
	M3	220	6,2	8,6	13,1	176,6	10	0	5	24,1	132,6	284	468	210000	4200	0	300
	M4	359,5	8,3	12,5	16,8	300,9	15	0	8	37,6	184,1	326	435	210000	4200	0	530
Aribert et al. [6]	1.1	240	6,2	9,8	15	190,4	N/A	N/A	N/A	40,0	164,0	367	–	210000	4200	0	380
	2,1	240	6,2	9,8	15	190,4	N/A	N/A	N/A	40,0	164,0	425	–	210000	4200	0	340
	3.1	230	7,5	12	21	164	N/A	N/A	N/A	40,0	205,0	317	–	210000	4200	0	483
	4,1	290	8,5	14	27	208	N/A	N/A	N/A	40,0	245,0	357	–	210000	4200	0	660
	5.1	490	12	23	27	390	N/A	N/A	N/A	40.0	290.0	286	–	210000	4200	0	980
Aribert et al. [6]	MH1	135,5	5,7	8,8	11,8	94,3	10	0	7	29,8	132,8	484	578	210000	4200	0	365
	MH2	154,3	6,7	10	13,4	107,5	10	0	7	29,8	146,8	481	608	210000	4200	0	530
	MH3	154,3	6,6	10	13,6	107,1	10	0	7	29,8	147,8	475	603	210000	4200	0	522
	MH4	195,9	7,7	11,2	18,2	137,1	10	0	7	29,8	176,8	542	640	210000	4200	0	760
	MH5	196,2	7,8	11,3	18,6	136,4	10	0	7	29,8	179,3	542	640	210000	4200	0	740
	MH6	189,5	5,7	8,4	19,8	133,1	10	0	7	29,8	170,8	610	697	210000	4200	0	402
	MH7	285	6,8	11,7	26,7	208,2	10	0	7	29,8	221,8	544	656	210000	4200	0	588
	MH8	238,6	6,1	10,6	14,3	188,8	10	0	7	29,8	154,3	566	671	210000	4200	0	454
	MH9	357,5	6,6	11,5	15,6	303,3	15	0	9	40,5	176,0	524	635	210000	4200	0	490
Aribert et al. [6]	MH10	154,5	6,7	10,1	13,6	107,1	10	10	7	49,8	168,3	481	608	210000	4200	0	580
	MH11	154,5	6,7	10	13,7	107,1	10	15	7	59,8	178,3	481	608	210000	4200	0	620
	MH12	154,5	6,7	10	13,7	107,1	10	20	7	69,8	188,3	481	608	210000	4200	0	664
Kuhlmann et al. [8]	A1	230,5	8,25	12,05	21	164,4	20	0	0	20,0	185,3	287	523,8	210000	4200	0.67	464,64
	A2	230,5	8,22	12,06	21	164,38	20	0	0	20,0	185,3	287	523,8	210000	4200	0.6	453,29
	A3	230,5	8,19	12,03	21	164,44	20	0	0	20,0	185,2	287	523,8	210000	4200	0	531,51
	A4	229,7	7,95	11,32	21	165,06	20	0	0	20,0	181,6	275	501,9	210000	4200	0.11	480,47
	A5	229,9	7,95	11,19	21	165,52	20	0	0	20,0	181,0	275	501,9	210000	4200	0.23	447,19
	A6	229,9	8,01	11,3	21	165,3	20	0	0	20,0	181,5	275	501,9	210000	4200	0.34	467,06
	A7	230,2	8,16	11,23	21	165,74	20	0	0	20,0	181,2	275	501,9	210000	4200	0.49	455,17
	A8	228,9	8,04	11,25	21	164,4	20	0	0	20,0	181,3	275	501,9	210000	4200	0	492,47
	B1	244,5	10	16,25	21	170	20	0	0	20,0	206,3	290	470,9	210000	4200	0	755,21
	B2	244.4	9.98	16.23	21	169.94	20	0	0	20.0	206.2	290	470.9	210000	4200	0.47	678.09
	B3	244,3	10,02	16,19	21	169,92	20	0	0	20,0	206,0	290	470,9	210000	4200	0.66	629,12
	B4	239,3	10,81	16,65	21	164	20	0	0	20,0	208,3	277	490,3	210000	4200	0.12	909,9
	B5	239.3	10.87	16.7	21	163.9	20	0	0	20.0	208.5	277	490.3	210000	4200	0.26	873.71
	B6	239,3	10.82	16,67	21	163,96	20	0	0	20,0	208,4	277	490,3	210000	4200	0.38	842,05
	B7	239,3	10,85	16,64	21	164,02	20	0	0	20,0	208,2	277	490,3	210000	4200	0.61	788,06
	B8	239.4	10.94	16.72	21	163.96	20	0	0	20.0	208.6	277	490,3	210000	4200	0	953,2
Robust,.., [9]	CWC	179,76	5,29	7,81	9,5	145,14	8,5	0	5	22,6	109,2	435,45	545,16	210000	4200	0	254,32

Published in : Thin-Walled Structures (2022), vol. 180, 109848
DOI: 10.1016/j.tws.2022.109848
Status : Postprint (Author's version)

Table 2

Database (continued) — EN 1993-1-8 model (K_{ini} & $F_{c,wc,Rk}$).

EXPERIMENTAL DATA		EN 1993-1-8 MODEL								
Reference		Elastic stiffness	Plastic resistance							
#0	#1	#18	#19	#20	#21	#22	#23	#24	#25
Author	Specimen	K_{ini} (kN/mm) *Eq. (1)*	ω (-)	k_{wc} (-) *Eq. (7)*	$\bar{\lambda}_p$ (-) *Eq. (9)*	Post-plastic $(\bar{\lambda}_p \leq 0.67)$ *Eq. (8)*	Elasto-plastic $(\bar{\lambda}_p > 0.67)$ *Eq. (8)*	$F_{c,wc,Rk}$ (kN) *Eq. (6)*	$F_{c,wc,Rk}/F_{Ru}$ (-)
Aribert et al. [6]	L1	1612	1	1	0.60	✓	–	323	N/A
	L2	1867	1	1	0.64	✓	–	545	N/A
	L3	1924	1	1	0.74	–	✓	706	0.81
	L4	1882	1	1	0.65	✓	–	377	N/A
	L5	2001	1	1	0.67	✓	–	584	N/A
	L6	2106	1	1	0.68	–	✓	609	0.74
	L7	2124	1	1	0.77	–	✓	757	0.86
Aribert... [6]	N1	2009	1	1	0.57	✓	–	391	N/A
Aribert et al. [6]	T1	2198	1	1	0.64	✓	–	531	N/A
	T2	2297	1	1	0.65	✓	–	555	N/A
	T3	2395	1	1	0.66	✓	–	579	N/A
	T4	2593	1	1	0.69	–	✓	618	0.66
Aribert et al. [6]	M1	628	1	1	0.72	–	✓	142	0.81
	M2	1343	1	1	0.95	–	✓	455	0.75
	M3	685	1	1	0.85	–	✓	204	0.68
	M4	747	1	1	1.04	–	✓	377	0.71
Aribert et al. [6]	1.1	785	1	1	1.11	–	✓	269	0.71
	2.1	785	1	1	1.19	–	✓	295	0.87
	3.1	1378	1	1	0.89	–	✓	414	0.86
	4.1	1472	1	1	1.02	–	✓	571	0.87
	5.1	1312	1	1	0.96	–	✓	797	0.81
Aribert et al. [6]	MH1	1180	1	1	0.88	–	✓	313	0.86
	MH2	1345	1	1	0.84	–	✓	417	0.79
	MH3	1339	1	1	0.84	–	✓	406	0.78
	MH4	1460	1	1	0.96	–	✓	594	0.78
	MH5	1507	1	1	0.95	–	✓	613	0.83
	MH6	1075	1	1	1.33	–	✓	373	0.93
	MH7	1065	1	1	1.50	–	✓	467	0.79
	MH8	733	1	1	1.35	–	✓	330	0.73
	MH9	563	1	1	1.63	–	✓	323	0.66
Aribert et al. [6]	MH10	1548	1	1	0.89	–	✓	457	0.79
	MH11	1640	1	1	0.92	–	✓	475	0.77
	MH12	1732	1	1	0.95	–	✓	493	0.74
Kuhlmann et al. [8]	A1	1367	1	1	0.73	–	✓	420	0.90
	A2	1362	1	1	0.73	–	✓	417	0.92
	A3	1356	1	1	0.73	–	✓	415	0.78
	A4	1286	1	1	0.73	–	✓	379	0.79
	A5	1278	1	1	0.73	–	✓	377	0.84
	A6	1293	1	1	0.73	–	✓	383	0.82
	A7	1311	1	1	0.72	–	✓	393	0.86
	A8	1303	1	1	0.72	–	✓	385	0.78
	B1	1783	1	1	0.65	✓	–	598	N/A
	B2	1780	1	1	0.65	✓	–	597	N/A
	B3	1785	1	1	0.65	✓	–	599	N/A
	B4	2018	1	1	0.58	✓	–	624	N/A
	B5	2033	1	1	0.58	✓	–	628	N/A
	B6	2021	1	1	0.58	✓	–	625	N/A
	B7	2025	1	1	0.58	✓	–	626	N/A
	B8	2046	1	1	0.57	✓	–	632	N/A
Robust... [9]	CWC	585	1	1	1.01	–	✓	195	0.77

Published in : Thin-Walled Structures (2022), vol. 180, 109848
DOI: 10.1016/j.tws.2022.109848
Status : Postprint (Author's version)

3. Formulae for the characterization of the CWC resistance

3.1. IMPROVED PLASTIC RESISTANCE F_{Rpl}

The evaluation of the reduced slenderness factor $\bar{\lambda}_p$ through **Eq. (9)**, of the reduction factor ρ through **Eq. (8)** and of the stress interaction factor k_{wc} through **Eq. (7)** raises few comments and questions, which will be addressed in the present section.

***Regarding the reduced plate slenderness* factor** $\bar{\lambda}_p$, it may be evaluated through **Eq. (10)** as the square root of the ratio between the plastic resistance of the plate $F_{Rpl(\rho=1.0)}$ (disregarding instability aspects) and the elastic critical instability load F_{cr}:

$$\bar{\lambda}_p = \sqrt{\frac{F_{Rpl(\rho=1.0)}}{F_{cr}}} \qquad (10)$$

In [9], where the use of **Eq. (9)** was suggested, the following Timoshenko formula was selected to evaluate F_{cr} [13], where υ designates the steel Poisson's ratio and k_{cr} is a buckling coefficient which depends on the geometry, loading and boundary conditions of the plate:

$$F_{cr} = k_{cr} \cdot \frac{\pi^2 \cdot E \cdot t_{wc}^3}{12 \cdot (1-\nu^2) \cdot d_c} \qquad (11)$$

For the determination of a precise value of k_{cr}, a rational buckling analysis [14] could be performed, as it becomes an accepted practice in international specifications [15]. However, in the present paper, the derivation of a simple analytical expression is sought. Therefore, reference is made to [16], where the following values of k_{cr} are proposed for a column profile such as the one presented in **Fig. 5**, for which the dimension ''a'' perpendicular to the transverse compression forces is assumed to be large with respect to the clear depth ''b'' of the column profile:

- $k_{cr} = \frac{4}{\pi}$ if the column web is subjected to two equal but opposite forces and is assumed to be simply connected to the flanges (no rotational restraint), see **Fig. 5**(d).
- $k_{cr} = \frac{8}{\pi}$ if the column web is subjected to two equal but opposite forces and is assumed to be rigidly connected to the flanges (full rotational restraint), see **Fig. 5**(f).

Through investigations considering the application of the software EBPlate [17] and the use of simple expressions for elastic critical resistances provided by Galéa in [16], the first value here above may be confirmed, but the second one appears to be too conservative. For the latter, a closer but still safe estimation may be suggested:

- $k_{cr} = \frac{14}{\pi}$ if the column web is subjected to two equal but opposite forces and is assumed to be rigidly connected to the flanges (full rotational restraint), see **Fig. 5**(f).

The same approach has also been used to define the values of the buckling coefficient k_{cr} for other support conditions and loading situations:

- $k_{cr} = \frac{7}{\pi}$ if the column web is subjected to a transverse force on one side only and is assumed to be simply connected to the flanges (no rotational restraint), see **Fig. 5**(e).

Published in : Thin-Walled Structures (2022), vol. 180, 109848
DOI: 10.1016/j.tws.2022.109848
Status : Postprint (Author's version)

- $k_{cr} = \frac{24}{\pi}$ if the column web is subjected to a transverse force on one side only and is assumed to be rigidly connected to the flanges (full rotational restraint), see **Fig. 5**(e).

Eq. (9) is based on the selection of a plate buckling coefficient $k_{cr} = 4/\pi$ (double-sided compression and simple supports). This may be seen as a safe approach as this represents the most severe loading situation. As a result, a less conservative approach could be followed for a single-sided compression force or double-sided compression forces with unequal intensities. This could lead to a higher level of accuracy of **Eq. (9)** in these specific situations.

Similarly, regarding the support conditions, the assumption of ''simple supports'' may also be questioned. For thick plates characterized by a low web slenderness, this assumption seems valid, as instability occurs beyond the yielding of the plate. However, for slender plates characterized by a high web slenderness, instability is known to occur in the elastic field and the influence of plasticity becomes quite limited. No or very few yielding is reported in the web at the root radius for a rolled section or at the toe of the weld for a welded section. As a consequence, the web can be assumed to be fully restrained by the flanges at its supports, and the value of the buckling coefficient k_{cr} can be updated, i.e. k_{cr} = 14/π can be used instead of k_{cr} = 4/π. Consequently, the new expression of the web slenderness ratio $\bar{\lambda}_{p,restr}$, which accounts for the improved boundary conditions, can be expressed through **Eq. (12)**:

$$\bar{\lambda}_{p,restr} = \sqrt{\frac{\omega \cdot k_{wc} \cdot b_{eff,c,wc} \cdot t_{wc} \cdot f_{y,wc}}{\frac{14}{\pi} \cdot \frac{\pi^2 \cdot E \cdot t_{wc}^3}{12 \cdot (1-\nu^2) \cdot d_c}}}$$

$$= \frac{1}{\sqrt{3.5}} \cdot 0.932 \cdot \sqrt{\frac{w \cdot k_{wc} \cdot b_{eff,c,wc} \cdot d_c \cdot f_{y,wc}}{E \cdot t_{wc}^2}} = 0.534 \cdot \bar{\lambda}_p \qquad (12)$$

Regarding the reduction factor ρ used in EN 1993-1-8, it is provided by the well-known Winter formula (with the correction introduced in Section 2.2), as expressed through **Eq. (8)**. By contrast, in Eurocode 3 Part 1–5 (EN 1993-1-5, see [18]) devoted to the design of plated structural elements, another expression is used in the chapter dedicated to patch loading (see **Eq. (13)**):

$$\rho = \begin{cases} 1.0 \;\; if \; \bar{\lambda}_p \leq 0.50 \\ \frac{0.5}{\bar{\lambda}_p} \; if \; \bar{\lambda}_p > 0.50 \end{cases} \qquad (13)$$

Both **Eqs. (8)** and **(13)** differ from each other by their shape but also by the length of their yield plateau (see **Fig. 6**). Based on comparisons with experimental tests (topic addressed in Section 3.3), it may be shown that none of them is fully satisfactory. Therefore, a new formula is proposed, see **Eq. (14)**, and compared to **Eqs. (8)** and **(13)** in **Fig. 6**.

$$\rho = \begin{cases} 1.0 \qquad if \; \bar{\lambda}_p \leq 0.50 \\ \frac{0.75}{\bar{\lambda}_p + 0.25} \; if \; \bar{\lambda}_p > 0.50 \end{cases} \qquad (14)$$

Published in : Thin-Walled Structures (2022), vol. 180, 109848
DOI: 10.1016/j.tws.2022.109848
Status : Postprint (Author's version)

Hence, the corresponding instability reduction factor ρ_{restr}, accounting for the improved boundary conditions, may be expressed by **Eq. (15)**:

$$\rho_{restr} = \begin{cases} 1.0 & if\ \bar{\lambda}_{p,restr} \leq 0.50 \\ \frac{0.75}{\bar{\lambda}_{p,restr}+0.25} & if\ \bar{\lambda}_{p,restr} > 0.50 \end{cases} \qquad (15)$$

Regarding the reduction factor k_{wc}, it was shown, through comparisons with the test results presented in **Table 2**, that **Eq. (7)** should be readjusted. The new suggested expression for this parameter is given by **Eq. (16)**:

$$k_{wc}^{*} = \begin{cases} 1.0 & when\ \sigma_n \leq 0.5 \cdot f_{y,wc} \\ 1.5 - \frac{\sigma_n}{f_{y,wc}} & when\ \sigma_n > 0.5 \cdot f_{y,wc} \end{cases} \qquad (16)$$

Finally, the new formula for the plastic resistance F_{Rpl} to instability can be expressed through **Eq. (17)**:

$$F_{Rpl} = \omega \cdot k_{wc}^{*} \cdot \rho_{restr} \cdot b_{eff,c,wc} \cdot t_{wc} \cdot f_{y,wc} \leq F_{Rpl(\rho=1.0)} \qquad (17)$$

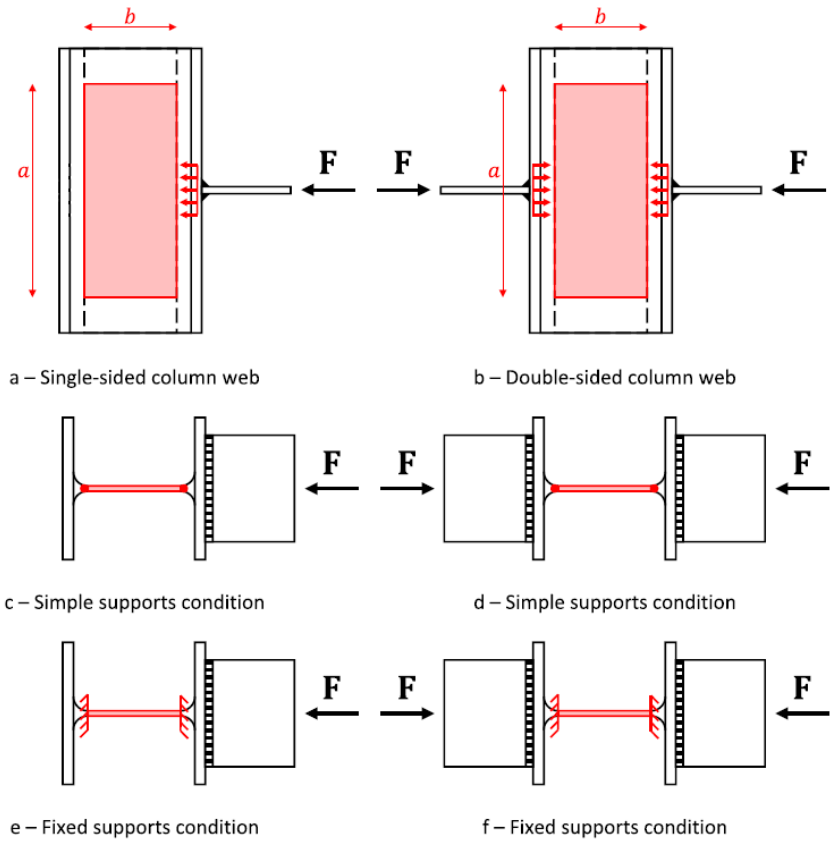

Fig. 5. Definition of the CWC support conditions.

Published in : Thin-Walled Structures (2022), vol. 180, 109848
DOI: 10.1016/j.tws.2022.109848
Status : Postprint (Author's version)

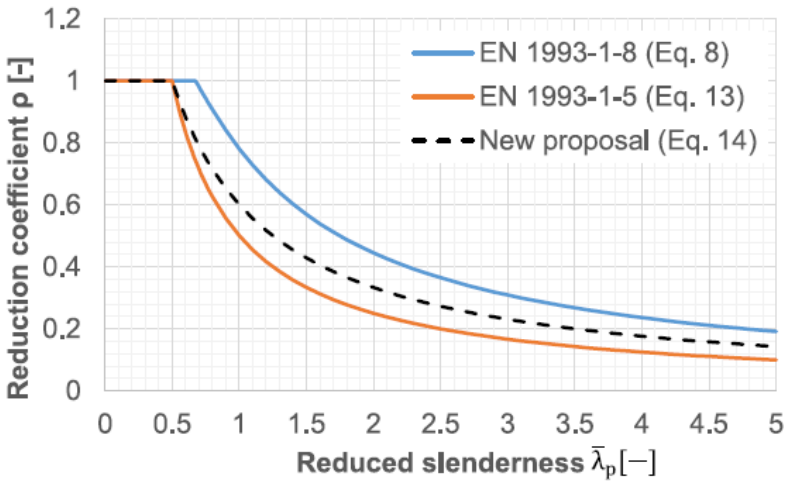

Fig. 6. Selection of an appropriate expression for the reduction factor ρ.

3.2. ULTIMATE RESISTANCE F_{Ru}

For sake of continuity and consistency, it is proposed to use for the ultimate resistance of the CWC a similar formalism as for **Eq. (17)**. This is expressed through **Eq. (18)**, where $f_{u,wc}$ is the ultimate material strength of the column web and where the subscript ''pp'' refers to the post-plastic range (i.e. the strain-hardening range) to which this formula applies:

$$F_{Ru,pp} = \omega \cdot k_{wc}^{*} \cdot \rho_u \cdot b_{eff,c,wc} \cdot t_{wc} \cdot f_{u,wc} \leq F_{Ru,pp(\rho_u=1.0)} \quad (18)$$

In **Eq. (18)**, ρ_u is the reduction factor which accounts for the risk of web instability. It can be defined, in agreement with what has been discussed in Section 3.1 (see **Eq. (15)**), through **Eq. (19)**, where $\bar{\lambda}_{pu}$ is the reduced slenderness factor and may be expressed through **Eq. (20)**. **Eq. (20)** was derived on the assumption of simple supports, similarly to **Eq. (9)**. This is due to the fact that the yielding of the web under transverse compression stresses at the root radius in a hot-rolled section or at the toe of the weld in a welded section modifies the support conditions of the column web from fixed supports to hinges.

$$\rho_u = \begin{cases} 1.0 & if\ \bar{\lambda}_{pu} \leq 0.50 \\ \frac{0.75}{\bar{\lambda}_{pu}+0.25} & if\ \bar{\lambda}_{pu} > 0.50 \end{cases} \quad (19)$$

$$\bar{\lambda}_{pu} = 0.932 \cdot \sqrt{\frac{\omega \cdot k_{wc}^{*} \cdot b_{eff,c,wc} \cdot d_c \cdot f_{u,wc}}{E \cdot t_{wc}^2}} = \bar{\lambda}_p \cdot \sqrt{\frac{f_{u,wc}}{f_{y,wc}}} \quad (20)$$

Eq. (18) is illustrated in **Fig. 7** for a specific value of $f_{u,wc} = 1.20 \cdot f_{y,wc}$ (see the blue curve). Its field of application is in the following range: $F_{ru}/F_{Rpl(\rho_{restr}=1.0)} > 1.0$ (i.e. ''post-plastic'' zone).

However, for high web slenderness, instability is known to occur in the elastic field before the development of any strain-hardening in the column web. In this domain, the ultimate resistance equals the plastic resistance and **Eq. (17)** applies, see **Eq. (21)**. The subscript ''ep'' in **Eq. (21)** refers to the fact

Published in : Thin-Walled Structures (2022), vol. 180, 109848
DOI: 10.1016/j.tws.2022.109848
Status : Postprint (Author's version)

that **Eq. (21)** applies to slenderness ranges where no benefit from strain-hardening may be expected, i.e. the steel material remains in the elasto-plastic range.

$$F_{Ru,ep} = F_{Rpl} = \omega \cdot k_{wc}^{*} \cdot \rho_{restr} \cdot b_{eff,c,wc} \cdot t_{wc} \cdot f_{y,wc} \leq F_{Rpl(\rho_{restr}=1.0)} \qquad (21)$$

Eq. (21) is illustrated in **Fig. 7** for a specific value of $f_{u,wc} = 1.20 \cdot f_{y,wc}$ (see the orange curve). Its field of application is in the following range: $F_{Ru}/F_{Rpl(\rho restr=1.0)} \leq 1.0$ (''elasto-plastic'' zone).

At the end, the ultimate resistance F_{Ru} of column webs under transverse compression may be simply expressed through **Eq. (22)**, as the maximum of **Eqs. (18)** and **(21)**:

$$F_{Ru} = \max\left(F_{Ru,pp}; F_{Ru,ep}\right) \qquad (22)$$

Eq. (22) is represented in **Fig. 7** by the envelope curve (see the dashed black curve). In **Fig. 7**, the limit value in between the ''elasto-plastic'' and the ''strain-hardening'' zones is the $\bar{\lambda}_{p,lim}$ slenderness factor. It is evaluated through **Eq. (23)** as the reduced slenderness at which **Eqs. (18)** and **(21)** provide equal resistances:

$$\bar{\lambda}_{p,lim} = \begin{cases} \dfrac{0.75 \cdot \frac{f_{u,wc}}{f_{y,wc}} - 0.25}{\sqrt{\frac{f_{u,wc}}{f_{y,wc}}}} & if \ \dfrac{f_{u,wc}}{f_{y,wc}} \leq 2.172 \\ \dfrac{0.25 \cdot \left(\frac{f_{u,wc}}{f_{y,wc}} - 1\right)}{\sqrt{\frac{f_{u,wc}}{f_{y,wc}}} - 0.534 \cdot \frac{f_{u,wc}}{f_{y,wc}}} & if \ \dfrac{f_{u,wc}}{f_{y,wc}} > 2.172 \end{cases} \qquad (23)$$

As the probability to have a steel material with a $f_{u,wc}/f_{y,wc}$ value higher than 2.172 is quite low, one can, practically speaking, simplify **Eq. (23)** into **Eq. (24)**:

$$\bar{\lambda}_{p,lim} = \frac{0.75 \cdot \frac{f_{u,wc}}{f_{y,wc}} - 0.25}{\sqrt{\frac{f_{u,wc}}{f_{y,wc}}}} \qquad (24)$$

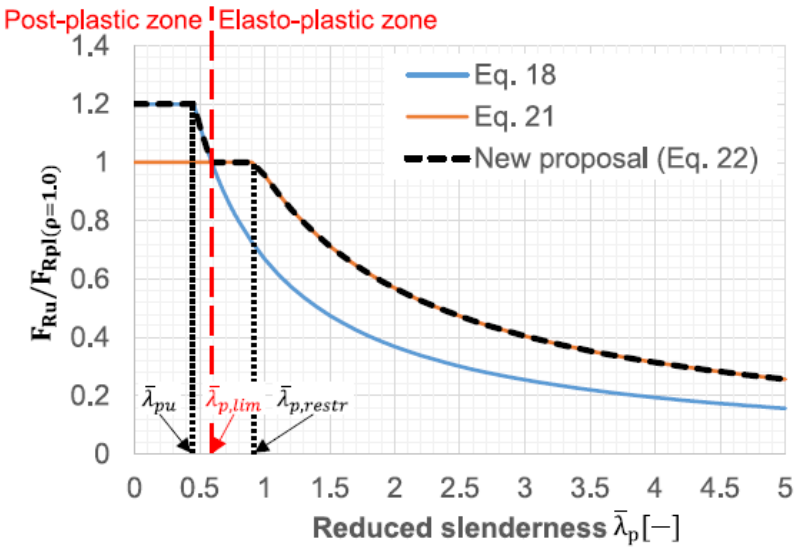

Fig. 7. Proposal for the evaluation of the CWC ultimate resistance.

Published in : Thin-Walled Structures (2022), vol. 180, 109848
DOI: 10.1016/j.tws.2022.109848
Status : Postprint (Author's version)

3.3. VALIDATION AND CONCLUSIONS

In **Table 1**, the ultimate strength of the material f_u is only reported for 38 tests out of 50. Consequently, the comparison between the experimental results and the analytical formulae developed in Section 3.2 for the ultimate resistance will be focussed on these tests only. **Table 3** gives an overview of these comparisons for the 38 relevant tests which are highlighted in light blue.

Except for test MH6, a very close agreement between the experimental and analytical values of the ultimate resistance may be observed (see the column #39). The safe character of the predictions may also be pointed out (i.e. the ratio $F_{Ru}/F_{Ru,exp}$ being lower than 1.0, with a mean value of 0.91 and standard deviation of 0.09). Some questions may reasonably be raised about the rather low experimental load for MH6, comparatively to the other tests, but as no precise explanation was found which could explain it, this test has been kept in **Table 3**.

Regarding the plastic resistance F_{Rpl}, it may be defined, in accordance with what has been presented in Section 3.2, as the ultimate resistance that the column web would exhibit if all strain-hardening effects would be neglected; so it simply corresponds to the orange curve in **Fig. 7**. For low slenderness, the full plastic resistance of the web is reached while, for higher ones, instability limits the carrying capacity, but not as much as what is nowadays assumed in EN 1993-1-8 as the beneficial effect of rigid support conditions may be considered, using a ρ_{restr} reduction factor (see **Eq. (15)**) instead of the current ρ reduction factor considered in EN 1993-1-8 (see **Eq. (8)**).

In **Table 3**, the plastic resistance F_{Rpl} has been computed for all available experimental results (see the columns #26-#29). The values of the ratio $F_{Rpl}/F_{Ru,exp}$ are reported in column #31, even if it has no physical meaning, except for the columns in which the failure mode occurs in the elasto-plastic zone. In the other cases, the $F_{Rpl}/F_{Ru,exp}$ should be lower than 1.0. A quite interesting ratio is also presented in column #30, i.e. $F_{Rpl}/F_{c,wc,Rk}$, which indicates the benefit provided by the new approach compared to the one proposed in EN 1993-1-8. A mean value of 1.09 is observed. This modification in the normative document would therefore allow to increase the design resistance of the column webs in compression by about 10%.

In addition, through a slight modification of the expression of the reduced slenderness in **Eq. (12)** (through the amendment of k_{cr} in **Eq. (11)**), even higher design values could be obtained in the case of a single-sided compression force or double-sided compression forces with unequal intensities, what would reflect the reality.

Published in : Thin-Walled Structures (2022), vol. 180, 109848
DOI: 10.1016/j.tws.2022.109848
Status : Postprint (Author's version)

Table 3

Database (continued) — Proposed model of component characterization (F_{Rpl} & F_{Ru})

EXPERIMENTAL DATA		PROPOSED MODEL OF COMPONENT CHARACTERISATION													
Reference		Plastic resistance						Ultimate resistance							
#0	#1	#26	#27	#28	#29	#30	#31	#32	#33	#34	#35	#36	#37	#38	#39
Author	Specimen	k_{wc}^* (-) Eq. (16)	$\bar{\lambda}_p$ (-) Eq. (9)	$\bar{\lambda}_{p,restr}$ (-) Eq. (12)	F_{Rpl} (kN) Eq. (17)	$F_{Rpl}/F_{c,wc,Rk}$ (-)	$F_{Rpl}/F_{Ru,exp}$ (-)	$\bar{\lambda}_{p,lim}$ (-) Eq. (24)	Post-plastic ($\bar{\lambda}_p \leq \bar{\lambda}_{p,lim}$)	Elasto-plastic ($\bar{\lambda}_p > \bar{\lambda}_{p,lim}$)	$\bar{\lambda}_{pu}$ (-) Eq. (20)	$F_{Ru,pp}$ (kN) Eq. (18)	$F_{Ru,ep}$ (kN) Eq. (21)	F_{Ru} (kN) Eq. (22)	$F_{Ru}/F_{Ru,exp}$ (-)
Aribert et al. [6]	L1	1	0,60	0,32	323	1,00	0,88	N/A	N/A	N/A	N/A	N/A	N/A	N/A	N/A
	L2	1	0,64	0,34	545	1,00	0,71	N/A	N/A	N/A	N/A	N/A	N/A	N/A	N/A
	L3	1	0,74	0,39	741	1,05	0,85	N/A	N/A	N/A	N/A	N/A	N/A	N/A	N/A
	L4	1	0,65	0,35	377	1,00	1,01	N/A	N/A	N/A	N/A	N/A	N/A	N/A	N/A
	L5	1	0,67	0,36	584	1,00	0,75	N/A	N/A	N/A	N/A	N/A	N/A	N/A	N/A
	L6	1	0,68	0,36	614	1,01	0,74	N/A	N/A	N/A	N/A	N/A	N/A	N/A	N/A
	L7	1	0,77	0,41	819	1,08	0,93	N/A	N/A	N/A	N/A	N/A	N/A	N/A	N/A
Aribert... [6]	N1	1	0.57	0.31	391	1.00	0.71	0.69	✓	–	0.69	**451**	391	451	0.82
Aribert et al. [6]	T1	1	0,64	0,34	531	1,00	0,70	0,73	✓	–	0,79	**593**	531	593	0,78
	T2	1	0,65	0,35	555	1,00	0,69	0,73	✓	–	0,81	**609**	555	609	0,76
	T3	1	0,66	0,35	579	1,00	0,69	0,73	✓	–	0,83	**626**	579	626	0,74
	T4	1	0,69	0,37	626	1,01	0,67	0,73	✓	–	0,86	**657**	626	657	0,70
Aribert et al. [6]	M1	1	0.72	0,39	147	1,04	0,84	0,67	–	✓	0,85	138	**147**	147	0,84
	M2	1	0,95	0,51	558	1,22	0,92	0,66	–	✓	1,11	425	**558**	558	0,92
	M3	1	0,85	0,45	234	1,14	0,78	0,77	–	✓	1,09	216	**234**	234	0,78
	M4	1	1,04	0,56	464	1,23	0,87	0,65	–	✓	1,20	343	**464**	464	0,87
Aribert et al. [6]	1.1	1	1.11	0,59	332	1,23	0,87	N/A	N/A	N/A	N/A	N/A	N/A	N/A	N/A
	2.1	1	1,19	0,64	365	1,24	1,07	N/A	N/A	N/A	N/A	N/A	N/A	N/A	N/A
	3.1	1	0,89	0,47	487	1,18	1,01	N/A	N/A	N/A	N/A	N/A	N/A	N/A	N/A
	4.1	1	1,02	0,54	701	1,23	1,06	N/A	N/A	N/A	N/A	N/A	N/A	N/A	N/A
	5.1	1	0,96	0,51	976	1,22	1,00	N/A	N/A	N/A	N/A	N/A	N/A	N/A	N/A
Aribert et al. [6]	MH1	1	0,88	0,47	366	1,17	1,00	0,59	–	✓	0,96	271	**366**	366	1,00
	MH2	1	0,84	0,45	473	1,13	0,89	0,62	–	✓	0,94	377	**473**	473	0,89
	MH3	1	0,84	0,45	463	1,14	0,89	0,62	–	✓	0,95	367	**463**	463	0,89
	MH4	1	0,96	0,51	727	1,22	0,96	0,58	–	✓	1,04	506	**727**	727	0,96
	MH5	1	0,95	0,51	751	1,22	1,01	0,58	–	✓	1,03	524	**751**	751	1,01
	MH6	1	1,33	0,71	464	1,24	1,15	0,57	–	✓	1,42	305	**464**	464	1,15
	MH7	1	1,50	0,80	586	1,25	1,00	0,60	–	✓	1,65	391	**586**	586	1,00
	MH8	1	1,35	0,72	411	1,25	0,90	0,59	–	✓	1,47	275	**411**	411	0,90
	MH9	1	1,63	0,87	407	1,26	0,83	0,60	–	✓	1,79	271	**407**	407	0,83
Aribert et al. [6]	MH10	1	0,89	0,48	542	1,19	0,94	0,62	–	✓	1,00	410	**542**	542	0,94
	MH11	1	0,92	0,49	575	1,21	0,93	0,62	–	✓	1,03	424	**575**	575	0,93
	MH12	1	0,95	0,50	603	1,22	0,91	0,62	–	✓	1,06	438	**603**	603	0,91
Kuhlmann et al. [8]	A1	0,83	0,66	0,35	364	0,87	0,78	0,83	✓	–	0,90	**434**	364	434	0,94
	A2	0.9	0,69	0,37	393	0,94	0,87	0,83	✓	–	0,94	**453**	393	453	1,00
	A3	1	0,73	0,39	435	1,05	0,82	0,83	✓	–	0,99	**480**	435	480	0,90
	A4	1	0,73	0,39	397	1,05	0,83	0,83	✓	–	0,99	**437**	397	437	0,91
	A5	1	0,73	0,39	396	1,05	0,88	0,83	✓	–	0,99	**436**	396	436	0,98
	A6	1	0,73	0,39	400	1,04	0,86	0,83	✓	–	0,99	**443**	400	443	0,95
	A7	1	0,72	0,38	407	1,03	0,89	0,83	✓	–	0,97	**457**	407	457	1,00
	A8	1	0,72	0,39	401	1,04	0,81	0,83	✓	–	0,98	**447**	401	447	0,91
	B1	1	0,65	0,35	598	1,00	0,79	0,76	✓	–	0,83	**677**	598	677	0,90
	B2	1	0,65	0,35	597	1,00	0,88	0,76	✓	–	0,83	**674**	597	674	0,99
	B3	0,84	0,59	0,32	503	0,84	0,80	0,76	✓	–	0,76	**609**	503	609	0,97
	B4	1	0,58	0,31	624	1,00	0,69	0,81	✓	–	0,77	**812**	624	812	0,89
	B5	1	0,58	0,31	628	1,00	0,72	0,81	✓	–	0,77	**820**	628	820	0,94
	B6	1	0,58	0,31	625	1,00	0,74	0,81	✓	–	0,77	**813**	625	813	0,97
	B7	0,89	0,54	0,29	557	0,89	0,71	0,81	✓	–	0,72	**759**	557	759	0,96
	B8	1	0,57	0,31	632	1,00	0,66	0,81	✓	–	0,76	**830**	632	830	0,87
Robust... [9]	CWC	1	1.01	0,54	239	1,23	0,94	0,62	–	✓	1,13	171	**239**	239	0,94

4. Formulae for the characterization of the CWC deformation capacity

4.1. POST-PLASTIC STIFFNESS K_{pp}

As stated in Section 1, four key properties are used to characterize the non-linear response of a component in the form of a $F - \Delta$ curve, three of them being already known from the previous pages, i.e. K_{ini}, F_{Rpl} and F_{Ru}. A proposal for the evaluation of the last property, i.e. the post-plastic stiffness K_{pp}, was made in [19,20]; it may be quickly derived from the expression of the elastic initial stiffness

Published in : Thin-Walled Structures (2022), vol. 180, 109848
DOI: 10.1016/j.tws.2022.109848
Status : Postprint (Author's version)

K_{ini}, as given by **Eq. (25)**, where E_{pp} is the strain-hardening modulus of steel which may reasonably be taken equal to $E/50$:

$$K_{pp} = K_{ini} \cdot \frac{E_{pp}}{E} = k_{ini} \cdot E_{pp} \qquad (25)$$

This expression reflects rather well the reality for many different components but is seen to be inadequate for column webs in compression. This may be explained by the fact that plasticity primarily affects the web in the zone located directly below the flanges. By contrast, the internal part of the web remains longer in the elastic range because of the diffusion of the load-introduction stresses into the web. The increase of the force F beyond F_{Rpl} is therefore leading to a progressive extension/diffusion of strain-hardening inside the web and to the progressive reduction of the remaining elastic zone of the web.

An appropriate formula has therefore been derived which better covers the physical response of the web in the post-plastic range. This one is based on the physical model illustrated in **Fig. 8**.

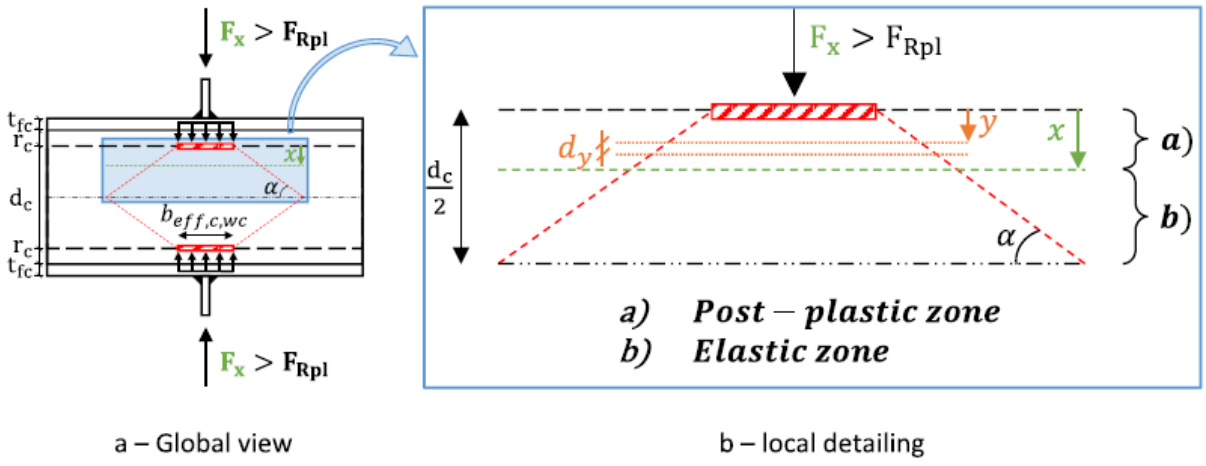

Fig. 8. Physical model for the prediction of K_{pp}.

In **Fig. 8**, the diffusion of the load-introduction stresses in the web is assumed to be linear over half of the web clear depth d_c, with a diffusion angle of α (see **Fig. 8**(a)). On half of the web, this model may be seen as a beam element in compression of depth $d_c/2$, of thickness t_{wc} and with a width varying from $b_{eff,c,wc}$ to $b_{eff,c,wc} + d_c \cdot \cot\alpha$. Assuming that, at a distance x (see **Fig. 8**(b)), the transverse stresses in the web just equal $f_{y,wc}$, the corresponding applied force may be expressed through **Eq. (26)**:

$$F_x = \left[b_{eff,c,wc} + 2 \cdot x \cdot \cot\alpha\right] \cdot t_{wc} \cdot f_{y,wc} \qquad (26)$$

When this force F_x, which is assumed to be higher than F_{Rpl}, applies:

- the web is assumed to be in the post-plastic zone over the depth x, and the material is therefore characterized by a value E_{pp} over this depth; the value of the transverse stress just under the flange is given by **Eq. (27)**;
- the web is assumed to behave elastically over the depth $d_c/2 - x$ and the material is characterized by the Young's modulus E.

$$f_{y,wc,x} = \frac{b_{eff,c,wc} + 2 \cdot x \cdot \cot\alpha}{b_{eff,c,wc}} \cdot f_{y,wc} \qquad (27)$$

Published in : Thin-Walled Structures (2022), vol. 180, 109848
DOI: 10.1016/j.tws.2022.109848
Status : Postprint (Author's version)

Consequently, the total shortening Δ of half a web under F_x may be expressed through **Eq. (28)** as the sum of two contributions:

- Δ_{el} which is the elastic shortening of the web over the depth $d_c/2$, and may be derived through **Eq. (29)**.
- $\Delta_{pp,x}$ which is the strain-hardening (i.e. post-plastic) shortening of the web over the depth x. It may be obtained by first considering the post-plastic shortening $d\Delta_{pp,x}$ of an infinitesimal slice dy of the web (see **Fig. 8**(b)). This infinitesimal shortening $d\Delta_{pp,x}$ may be easily derived, through the elastic beam theory, as expressed through **Eq. (30)**. The integration of this infinitesimal displacement over the depth x gives the post-plastic shortening $\Delta_{pp,x}$ of the web over the depth x (see **Eq. (31)**).

$$\Delta = \Delta_{el} + \Delta_{pp,x} \tag{28}$$

$$\Delta_{el} = \frac{F_x}{K_{ini}} = \frac{\left[b_{eff,c,wc} + 2 \cdot x \cdot cot\ \alpha\right] \cdot t_{wc} \cdot f_{y,wc}}{\frac{0.7 \cdot b_{eff,c,wc} \cdot t_{wc}}{d_c} \cdot E}$$

$$= \frac{\left[b_{eff,c,wc} + 2 \cdot x \cdot cot\ \alpha\right] \cdot d_c \cdot f_{y,wc}}{0.7 \cdot b_{eff,c,wc} \cdot E} = \frac{f_{y,wc,x} \cdot d_c}{0.7 \cdot E} \tag{29}$$

$$d\Delta_{pp,x} = \frac{F_x}{E_{pp} \cdot \left(b_{eff,c,wc} + 2 \cdot y \cdot \cot \alpha\right) \cdot t_{wc}} \cdot dy \tag{30}$$

$$\Delta_{pp,x} = \int_0^x d\Delta_{pp,x} = \frac{b_{eff,c,wc} \cdot f_{y,wc,x}}{2 \cdot E_{pp} \cdot \cot \alpha} \cdot$$

$$\times \left[\ln \left| b_{eff,c,wc} + 2 \cdot x \cdot cot\ \alpha \right| - \ln \left| b_{eff,c,wc} \right|\right] \tag{31}$$

The evolutions of the elastic shorting (i.e. "$2 \cdot \Delta_{el}$"), the post-plastic shortening (i.e. "$2 \cdot \Delta_{pp,x}$") and the total shortening of the web (i.e. "$2 \cdot \Delta$") for the test "$B6$" (given in **Table 1**) are presented in **Fig. 9**(a) for an increasing value of the applied force F (corresponding to an increasing value of x in the strain-hardening zone). In **Fig. 9**, the factor "2" affecting the stiffnesses and the displacements simply reflects that the force is applied symmetrically on both section flanges and therefore activates two CWC components.

In **Fig. 9**(a), the post-plastic stiffness appears as rather constant and, by sake of simplification, will be considered as such. The selected value of the linearized post-plastic approximation is shown in **Fig. 9**(b). It is obtained by:

- selecting the post-plastic shortening $\Delta_{pp,x}$ from **Eq. (31)** for the specific value of $x = d_c/2$ (see the value $2 \cdot \Delta_{pp,d_c/2}$ in **Fig. 9**(b));
- computing the increment of force $\Delta F = F_{x=d_c/2} - F_{x=0}$ which is responsible of the post-plastic shortening $\Delta_{pp,d/2}$, i.e. $\Delta F = b_{eff,c,wc} \cdot t_{wc} \cdot \left(f_{y,wc,d_c/2} - f_{y,wc}\right)$;
- deriving the post-plastic stiffness K_{pp} as the ratio between ΔF and $\Delta_{pp,d_c/2}$;

Published in : Thin-Walled Structures (2022), vol. 180, 109848
DOI: 10.1016/j.tws.2022.109848
Status : Postprint (Author's version)

- reporting the so-obtained stiffness from the point with coordinates $F = F_{Rpl}$ and $2\Delta = 0$, in accordance with **Fig. 2**.

As a result, the following expression of K_{pp} (see **Eq. (32)**) is proposed for a CWC component (i.e. a column web of depth $d_c/2$):

$$K_{pp} = \frac{2 \cdot E_{pp} \cdot t_{wc} \cdot (\mu - 1) \cdot \cot \alpha}{\mu \cdot \ln \mu} \quad (32)$$

where:

$$\mu = \frac{b_{eff,c,wc} + d_c \cdot \cot \alpha}{b_{eff,c,wc}} \quad (33)$$

Three estimations of K_{pp} are provided, respectively for three values of the diffusion angle α, i.e., 30°, 40° and 45°. These values are reported in **Table 4** for each individual test (see the columns #41, #42 and #43). In addition, the experimental curves for the tests *''A1''-''A8''* and *''B1''-''B8''* (highlighted in light blue in **Table 4**) are reported in **Fig. 10** (see the black curves), together with the analytical predictions of their four main mechanical properties (i.e. K_{ini}, K_{pp}, F_{Rpl} and F_{Ru}, these properties being highlighted in light grey in **Fig. 10**). From the visual comparisons between the experimental results and the three proposals for K_{pp} (see **Fig. 10**), it appears that the value of α = 40° fits well to the reality and it is here selected, so leading to the final expression of K_{pp}:

$$K_{pp} = \frac{2.384 \cdot E_{pp} \cdot t_{wc} \cdot (\mu - 1)}{\mu \cdot \ln \mu} \quad (34)$$

where:

$$\mu = \frac{b_{eff,c,wc} + 1.192 \cdot d_c}{d_{eff,c,wc}} \quad (35)$$

The visual comparisons are justified here by the fact that experimental values of $K_{pp,exp}$ are almost impossible to derive from the test results since, in most of the cases, early buckling prevents the development of a well-marked straight post-limit response, as it is the case, for instance, in the test ''B4'' (see **Fig. 10**(h)) and the test *''B8''* (see **Fig. 10**(p)). For the latter, a reasonable agreement is observed between the experimental and analytical values of K_{pp}.

On this basis, the CWC ultimate deformation capacity Δ_u may now be computed (see Section 4.2).

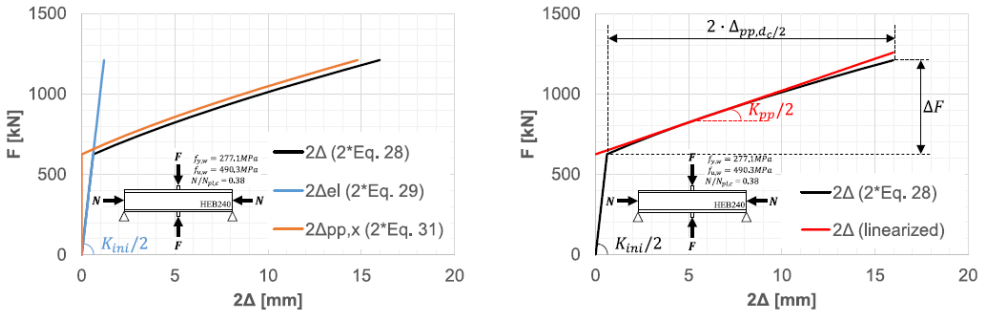

a – Non-linear curve

b – Non-linear curve and linear approximation

Fig. 9. *F - 2Δ* curve for the test B6 according to the physical model for the prediction of K_{pp}.

Published in : Thin-Walled Structures (2022), vol. 180, 109848
DOI: 10.1016/j.tws.2022.109848
Status : Postprint (Author's version)

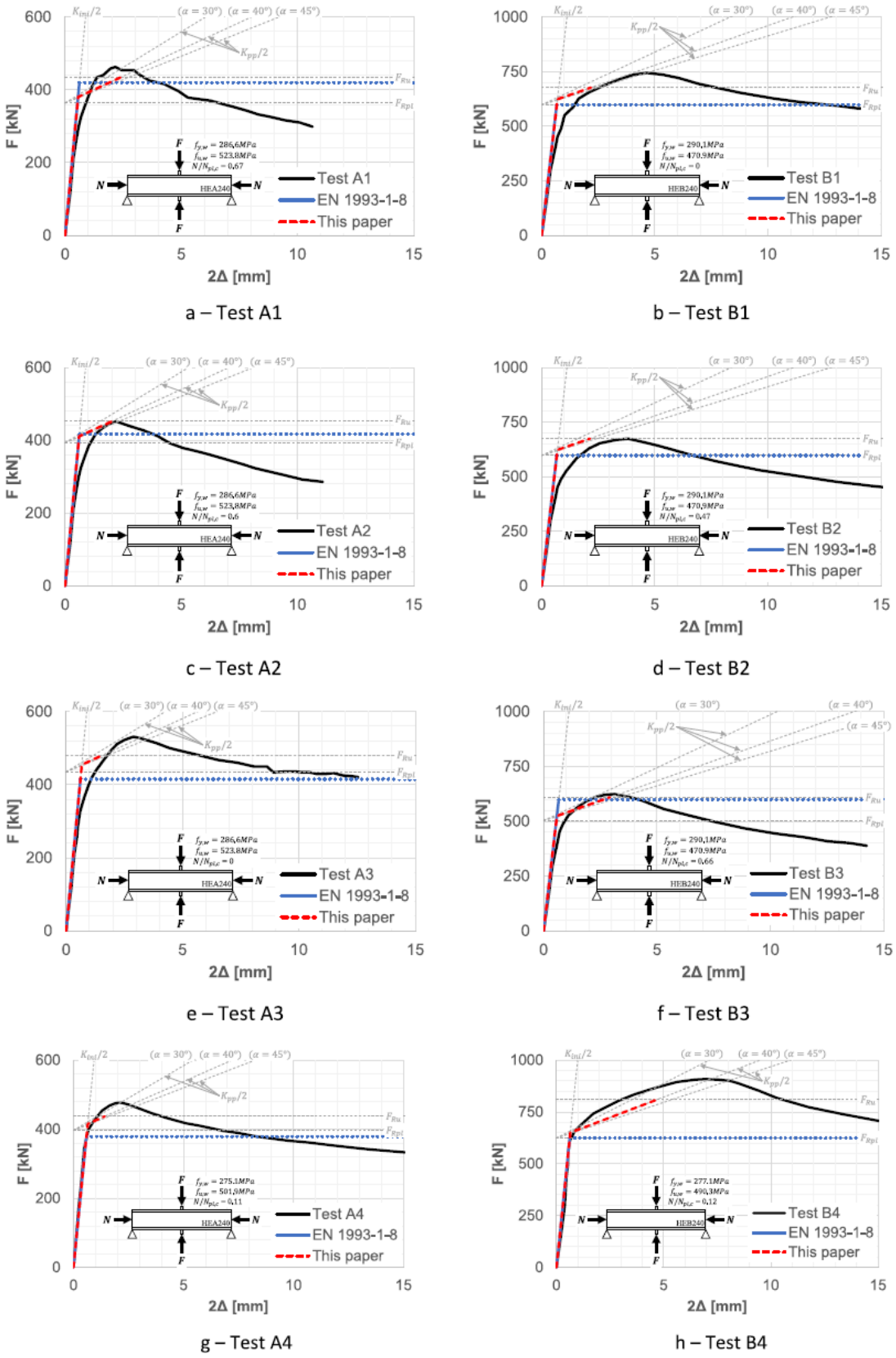

Fig. 10. Validation of the new proposed model against experimental results.

Published in : Thin-Walled Structures (2022), vol. 180, 109848
DOI: 10.1016/j.tws.2022.109848
Status : Postprint (Author's version)

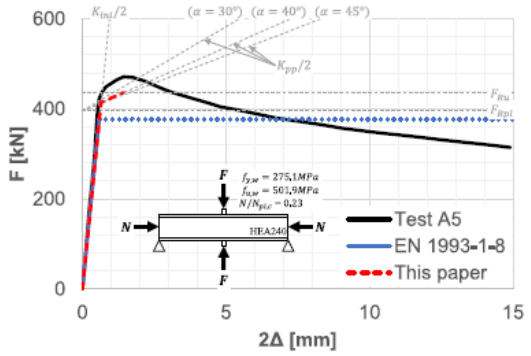

i – Test A5

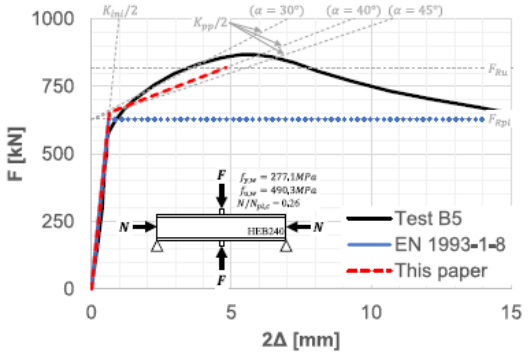

j – Test B5

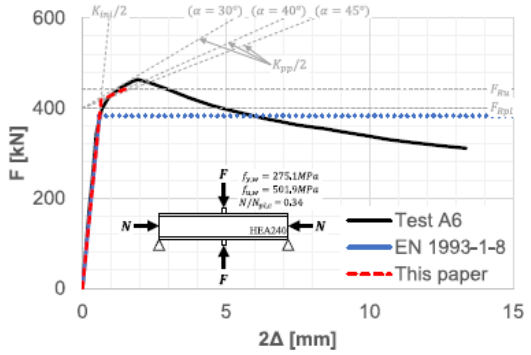

k – Test A6

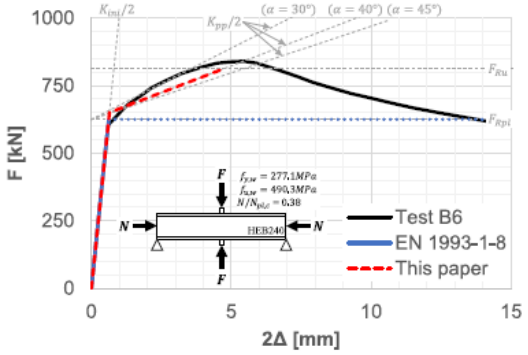

l – Test B6

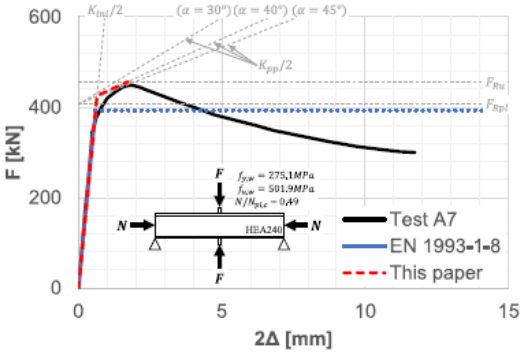

m – Test A7

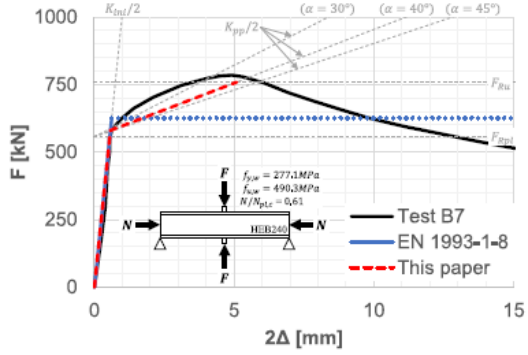

n – Test B7

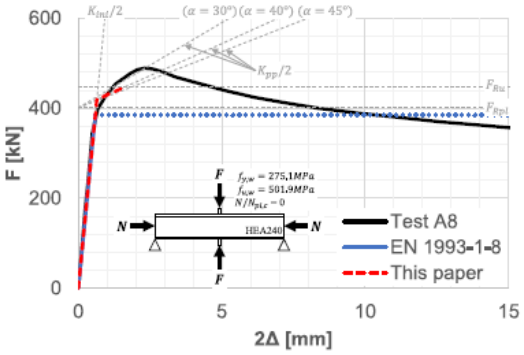

o – Test A8

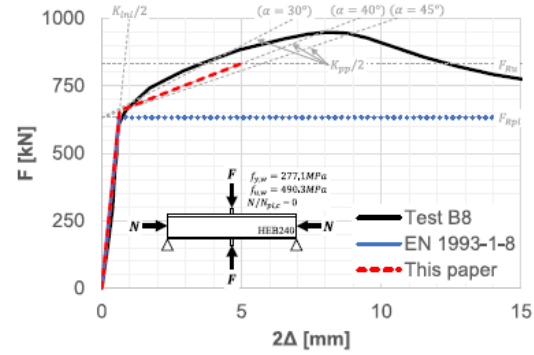

p – Test B8

Fig. 10. *(continued)*

Published in : Thin-Walled Structures (2022), vol. 180, 109848
DOI: 10.1016/j.tws.2022.109848
Status : Postprint (Author's version)

Table 4

Database (continued) – Proposed model of component characterization $(K_{ini}, K_{pp}$ & $\Delta_u)$.

EXPERIMENTAL DATA		PROPOSED MODEL OF COMPONENT CHARACTERISATION											
Reference		Elastic stiffness	Post-plastic stiffness			Ultimate deformation capacity						
#0	#1	#40	#41	#42	#43	#44	#45	#46	#47	#48	#49	#50
Author	Specimen	K_{ini} (kN/mm) *Eq. (1)*	$K_{pp,30°}$ (kN/mm) *Eq. (32)*	$K_{pp,40°}$ (kN/mm) *Eq. (34)*	$K_{pp,45°}$ (kN/mm) *Eq. (32)*	$2\Delta_{u,30°}$ (mm) *Eq. (36)*	$2\Delta_{u,40°}$ (mm) *Eq. (36)*	$2\Delta_{u,45°}$ (mm) *Eq. (36)*	$2\Delta_{u,exp}$ (mm)	$\Delta_{u,30°}/\Delta_{u,exp}$ (-)	$\Delta_{u,40°}/\Delta_{u,exp}$ (-)	$\Delta_{u,45°}/\Delta_{u,exp}$ (-)
Aribert et al. [6]	L1	1612	71.8	53.5	46.4	N/A	N/A	N/A	–	–	–	–
	L2	1867	90,1	67,4	58,5	N/A	N/A	N/A	–	–	–	–
	L3	1924	98.3	73.7	64.1	N/A	N/A	N/A	–	–	–	–
	L4	1882	74,3	55.1	47.7	N/A	N/A	N/A	–	–	–	–
	L5	2001	91,6	68,3	59,3	N/A	N/A	N/A	–	–	–	–
	L6	2106	92.7	69.0	59.8	N/A	N/A	N/A	–	–	–	–
	L7	2124	100.7	75.2	65.3	N/A	N/A	N/A	–	–	–	–
Aribert,.., [6]	N1	2009	83.7	62.2	53.8	1.44	1.93	2.23	–	–	–	–
Aribert et al. [6]	T1	2198	93,6	69,6	60,3	1,33	1,79	2,06	–	–	–	–
	T2	2297	94.5	70.2	60.7	1.16	1.56	1.80	–	–	–	–
	T3	2395	95.4	70.7	61.2	0.98	1.33	1.53	–	–	–	–
	T4	2593	97,0	71,7	62,0	0,63	0,85	0,98	–	–	–	–
Aribert et al. [6]	M1	628	44,6	33.9	29.7	0.47	0.47	0.47	–	–	–	–
	M2	1343	74,6	56,1	48,9	0,83	0,83	0,83	–	–	–	–
	M3	685	52.6	40.1	35.1	0.68	0.68	0.68	–	–	–	–
	M4	747	66.4	50.8	44.7	1.24	1.24	1.24	–	–	–	–
Aribert et al. [6]	1,1	785	54,7	41,5	36,3	N/A	N/A	N/A	–	–	–	–
	2.1	785	54.7	41.5	36.3	N/A	N/A	N/A	–	–	–	–
	3.1	1378	72.9	54.7	47.6	N/A	N/A	N/A	–	–	–	–
	4,1	1472	81,4	61,2	53,3	N/A	N/A	N/A	–	–	–	–
	5.1	1312	101.6	77.3	67.8	N/A	N/A	N/A	–	–	–	–
Aribert et al. [6]	MH1	1180	57,0	42,7	37,1	0,62	0,62	0,62	–	–	–	–
	MH2	1345	66.5	49.8	43.3	0.70	0.70	0.70	–	–	–	–
	MH3	1339	65.7	49.2	42.7	0.69	0.69	0.69	–	–	–	–
	MH4	1460	75,4	56,6	49,2	1,00	1,00	1,00	–	–	–	–
	MH5	1507	76.8	57.5	50.0	1.00	1.00	1.00	–	–	–	–
	MH6	1075	55.8	41.8	36.4	0.86	0.86	0.86	–	–	–	–
	MH7	1065	63,5	47,9	41,8	1,10	1,10	1,10	–	–	–	–
	MH8	733	53.0	40.3	35.3	1.12	1.12	1.12	–	–	–	–
	MH9	563	52.0	39.8	35.0	1.45	1.45	1.45	–	–	–	–
Aribert et al. [6]	MH10	1548	68.8	51.3	44.4	0.70	0.70	0.70	–	–	–	–
	MH11	1640	69.7	51.8	44.9	0.70	0.70	0.70	–	–	–	–
	MH12	1732	70,5	52,4	45,3	0,70	0,70	0,70	–	–	–	–
Kuhlmann et al. [8]	A1	1367	78,1	58,8	51,3	1,82	2,41	2,76	2,12	0,86	1,14	1,30
	A2	1362	77,8	58,6	51,1	1,56	2,07	2,37	2,21	0,70	0,94	1,07
	A3	1356	77,5	58,4	50,9	1,16	1,55	1,77	2,83	0,41	0,55	0,63
	A4	1286	74,8	56,4	49,2	1,08	1,43	1,64	1,94	0,56	0,74	0,84
	A5	1278	74,7	56,3	49,1	1,08	1,43	1,64	1,36	0,79	1,05	1,21
	A6	1293	75,3	56,8	49,5	1,14	1,52	1,74	1,86	0,61	0,82	0,94
	A7	1311	76,7	57,8	50,4	1,31	1,74	2,00	1,84	0,71	0,95	1,09
	A8	1303	75,7	57,1	49,8	1,21	1,60	1,84	2,31	0,52	0,69	0,80
	B1	1783	96,5	72,5	63,1	1,63	2,16	2,48	4,73	0,34	0,46	0,53
	B2	1780	96,3	72,4	63,0	1,61	2,14	2,46	3,28	0,49	0,65	0,75
	B3	1785	96,6	72,6	63,2	2,20	2,92	3,36	2,94	0,75	0,99	1,14
	B4	2018	105,5	79,2	68,9	3,56	4,75	5,46	7,01	0,51	0,68	0,78
	B5	2033	106,1	79,6	69,3	3,63	4,83	5,55	5,35	0,68	0,90	1,04
	B6	2021	105,6	79,2	68,9	3,57	4,76	5,47	5,05	0,71	0,94	1,08
	B7	2025	105,9	79,4	69,1	3,82	5,09	5,85	4,95	0,77	1,03	1,18
	B8	2046	106,8	80,1	69,7	3,70	4,93	5,66	8,30	0,45	0,59	0,68
Robust,.., [9]	CWC	585	44,9	34,2	30,0	0,82	0,82	0,82	–	–	–	–

4.2. ULTIMATE DEFORMATION CAPACITY Δ_u

The deformation capacity Δ_u is defined in Section 1. Its expression may be easily derived from **Fig. 2**(a), as expressed through **Eq. (36)**:

Published in : Thin-Walled Structures (2022), vol. 180, 109848
DOI: 10.1016/j.tws.2022.109848
Status : Postprint (Author's version)

$$\Delta_u = \max\left(\frac{F_{Ru} - F_{Rpl}}{K_{pp}}; \frac{F_{Ru}}{K_{ini}}\right) \quad (36)$$

Analytical predictions of $2 \cdot \Delta_u$ are reported in **Table 4** for each experimental test and for each investigated value of the diffusion angle α (see the columns #44, #45 and #46, respectively). In **Table 4**, the experimental ultimate deformation capacity $2 \cdot \Delta_{u,exp}$ is also reported for the 16 tests highlighted in light blue (see column #47). Comparisons between analytical predictions and experimental values are given in the columns #48, #49 and #50. They show a reasonable agreement especially with the diffusion angle α = 40° selected in the present article, knowing that the experimental values $\Delta_{u,exp}$ depend on the buckling resistance, which is itself highly influenced by the profile geometrical imperfections. This being, the accuracy of the analytical prediction Δ_u can be seen as rather aleatory. In the tests presented in **Fig. 10**, the proposed formula is seen to provide results which are either quite close, or lower than reality. In any cases, the predictions appear to be conservative.

4.3. $F - \Delta$ CURVE

The four key behavioural properties of the CWC component being known, the full $F - \Delta$ curve characterizing the CWC component can be drawn. In the present paper, the bilinear approach presented in **Fig. 2**(a) was applied but a more complex trilinear approach could be used (see **Fig. 2**(b)). The new analytical model is presented in **Fig. 4**(b) for the test *''CWC''* (see the dashed red curve) and in **Fig. 10** for the tests *"A1"-"A8"* and *"B1"-"B8"* (see the dashed red curves). Comparisons between experimental and analytical results show a good agreement in terms of both ultimate resistance and deformation capacity. From **Figs. 4** and **10**, two situations may be clearly contemplated:

- In **Fig. 4**, the column web of the test *''CWC''* is characterized by a high slenderness factor (i.e. $\bar{\lambda}_p > \bar{\lambda}_{p,lim}$ in **Table 3**). Consequently, it fails by buckling before the full plastic resistance of the web is reached, and therefore no plastic deformation capacity may be expected (i.e. $\Delta_u = \Delta_{pl}$ in **Fig. 2**(a) and the model exhibits a linear shape). This situation is also met for the experimental tests *''M1''-''M4''*, *''1.1''-''5.1''* and *''MH1''-''MH12''* reported in **Table 3**.
- In **Fig. 10**, the column web of the different tests is rather stocky ≤ and thus characterized by a low slenderness factor (i.e. $\bar{\lambda}_p \leq \bar{\lambda}_{p,lim}$ in **Table 3**). Consequently, a larger deformation capacity may be expected (i.e. $\Delta_u \neq \Delta_{pl}$ in **Fig. 2**(a) and the model exhibits a well-marked bilinear shape).

For sake of clarity, the current EN 1993-1-8 model was also reported in **Figs. 4** and **10** (see the solid blue curves with the infinite dotted plateau). Comparisons with the new analytical model proposed in the present paper clearly show that the latter outperforms the EN 1993-1-8 model by providing a more accurate prediction of the CWC $F - \Delta$ curve.

5. Conclusions

The CWC component influences a wide range of steel and composite beam-to-column connections, including welded and bolted ones. Design formulae are available in standards and codes, for instance in EN 19931-8. These formulae allow the prediction of the design resistance and the initial stiffness of

Published in : Thin-Walled Structures (2022), vol. 180, 109848
DOI: 10.1016/j.tws.2022.109848
Status : Postprint (Author's version)

this component, but no information is provided in terms of maximum deformation capacity and ultimate resistance. This information is however required as soon as plastic analysis with partial strength joints is addressed, or to assess the capacity of the structure to mitigate the risk of progressive collapse under exceptional events.

In the present paper, analytical expressions are provided and validated through comparisons with experimental results for the prediction of the maximum plastic deformation capacity of the component and for the determination of its ultimate resistance. These expressions are rather complex and would require further numerical investigations and simplifications before considering any introduction in modern design codes. However, they pave the way for the prediction of the CWC full-range behaviour.

As an outcome of this study, a refined and less conservative expression than the one proposed in EN 1993-1-8 is proposed for the evaluation of the design resistance of the CWC component.

CRediT authorship contribution statement

Jean-Pierre Jaspart: Writing – original draft, Validation, Supervision, Software, Methodology, Investigation, Formal analysis, Conceptualization. **Adrien Corman:** Writing – review & editing, Visualization, Validation, Software. **Jean-François Demonceau:** Writing – review & editing, Supervision.

Declaration of competing interest

The authors declare that they have no known competing financial interests or personal relationships that could have appeared to influence the work reported in this paper.

Data availability

No data was used for the research described in the article.

References

[1] European Committee for Standardization (CEN), Eurocode 3: Design of steel structures – part 1-8: Design of joints, in: Final Draft PrEN 1993-1-8. Brussels, Belgium, 2005.

[2] J.-P. Jaspart, K. Weynand, Design of Joints in Steel and Composite Structures, Wiley-VCH Verlag GmbH & Co. KGaA, Weinheim, Germany, 2016.

[3] S. Yan, K.J.R. Rasmussen, Generalised component method-based finite element analysis of steel frames, J. Constr. Steel Res. 187 (September) (2021).

[4] L. Simões Da Silva, A. Santiago, P. Vila Real, Post-limit stiffness and ductility of end-plate beam-to-column steel joints, Comput. Struct. 80 (5–6) (2002) 515–531.

[5] A.M. Coelho Girão, Characterization of the ductility of bolted end plate beam-to-column steel connections, no. July, 2004, p. 370.

[6] D. Beg, E. Zupančič, I. Vayas, On the rotation capacity of moment connections, J. Constr. Steel Res. 60 (3-5) (2004) 601–620.

[7] J.-P. Jaspart, Study of the Semi-Rigidity of Beam-To-Column Steel Joints and

Published in : Thin-Walled Structures (2022), vol. 180, 109848
DOI: 10.1016/j.tws.2022.109848
Status : Postprint (Author's version)

Influence of this Semi-Rigidity on the Strength and Stability of Steel Frames (in French) (Ph.D. thesis), University of Liège, Liège (Belgium), 1991.

[8] European Committee for Standardization, NBN EN 1993-1-1 – Eurocode 3 : Design of Steel Structures – Part 1-1 : General Rules and Rules for Buildings, Brussels, 2005.

[9] J.M. Aribert, A. Lachal, M. Moheissen, Interaction between local buckling and strength of a hot-rolled profile under to local double compression (steel grades up to FeE 460) (in french), Constr. Métall. (2) (1990) 3–23.

[10] J.-P. Jaspart, Recent Advances in the Field of Steel Joints; Column Bases and Further Configurations for Beam-To-Column Joints and Beam Splices (Professorship thesis), University of Liège, Liège (Belgium), 1997.

[11] F. Kühnemund, Verification of the Rotation Capacity of Joints in Steel Structures (in German) (Ph.D. thesis), University of Stuttgart, Stuttgart (Germany, 2003.

[12] U. Kuhlmann, et al., Robust Impact Design of Stel and Composite Building Structures, Final Report of the European Project RFCS 'Robustimpact', European Commission, Brussels, 2007.

[13] S.P. Timoshenko, J.M. Gere, Theory of Elastic Stability, second ed., 1966.

[14] V.V. Nguyen, G.J. Hancock, C.H. Pham, Analyses of thin-walled sections under localised loading for general end boundary conditions – Part 2: Buckling, Thin-Walled Struct. 119 (2016) (2017) 973–987.

[15] V.V. Nguyen, G.J. Hancock, C.H. Pham, Consistent and simplified direct strength method for design of cold-formed steel structural members under localized loading, J. Struct. Eng. 146 (6) (2020).

[16] Y. Galéa, Equilibrium bifurcation level of an unstiffened panel under transverse compression loads (in French), Constr. Métall. (1) (1984) 1–19.

[17] CTICM, Software EBPlate (version 2.01) - Evaluation of elastic critical buckling stresses for plates. France.

[18] European Committee for Standardization (CEN), Eurocode 3: Design of Steel Structures – Part 1-5: Plated Structural Elements, Final Draft PrEN 1993-1-5. Brussels, Belgium, 2003.

[19] J.-P. Jaspart, A. Corman, J.-F. Demonceau, Ductility assessment of structural steel and composite joints, in: SDSS 2019 - International Colloquium on Stability and Ductility of Steel Structures, 2019.

[20] J.-P. Jaspart, R. Maquoi, Prediction of the semi-rigid and partial-strength properties of structural joints, in: SSRS Annual Task Group Technical Session and Meeting, 1994, pp. 177–191.